This article has been accepted for publication in a future issue of this journal, but has not been fully edited. Content may change prior to final publication.

Memristive Behavior Observed in a Defected Single-Walled Carbon Nanotube

Adam W. Bushmaker, Chia-Chi Chang, Vikram V. Deshpande, Moh. R. Amer, Marc W. Bockrath, Stephen B. Cronin

***Abstract*—Memristive electrical behavior has recently gained attention because of technological advances in nanostructuring, which has enabled the fabrication of working devices. However, such investigations have been limited to mobile ionic systems, and memristive behavior in other types of nano-scale systems has been largely overlooked. Here, we report direct measurement of memristive behavior of defect states in a quasi-metallic, single-walled carbon nanotube (CNT) field-effect transistor (FET). After exposing the CNT FET to laser irradiation, the conductance-gate voltage profile (G-V_g) indicates the creation of a gate-tunable, resonant electron scattering defect. Once a defect is formed, current flowing in the forward and reverse directions reversibly switches the G-V_g characteristics of the device. The changes in conductance are attributed to current direction-sensitive changes in the structure of an isolated defect state in the nanotube. The defect scattering spectra are extracted from the G-V_g data using a Landauer model.**

***Index Terms*— Annealing, carbon nanotube (CNT), defects, lasers, memristive systems**

I. Introduction

A. Defects in Carbon nanotubes

The study of defects in carbon nanotubes (CNTs) has been driven by the desire to understand the effect of defects on the ideal conductance of CNTs [1-3], as well as several specific device applications, such as heterojunction devices joined by Stone-Wales (5-7) defects [4-6]. Choi et al. used *ab initio* methods to examine the results of atomic substitutional defects (doping), 5-7 defects, and vacancy defects on the density of states and conductivity of CNTs [7]. These defects were found to manifest themselves as resonant electron scattering centers, only affecting transport strongly at the defect energy. Experimental investigations have confirmed the resonant nature of these few-atom defects, by observing gate-voltage tunable resistance [8, 9]. Scanning tunneling microscopy (STM) studies have shown that defects can be reversibly created and annihilated in CNTs [10, 11].

B. Memristive Behavior

In this work, a defect is created with a focused laser spot in a suspended single-walled metallic CNT field effect transistor. The defect is observed in the room-temperature conductance-gate voltage characteristics (G-V_g) taken at low bias voltage (V_b). When high currents are passed through the CNT, changes are observed in the G-V_g relationship that depend on the direction of the current flow. This direction-sensitive current annealing behavior is associated with memristive systems [12-17], which is a general class of circuit elements that includes the memristor, the thermistor, and ionic systems in general. Memristors are considered to be the fourth circuit element (in addition to resistors, capacitors and inductors), and have a resistance that depends on the electrical history of the device and yet are incapable of storing energy [12].

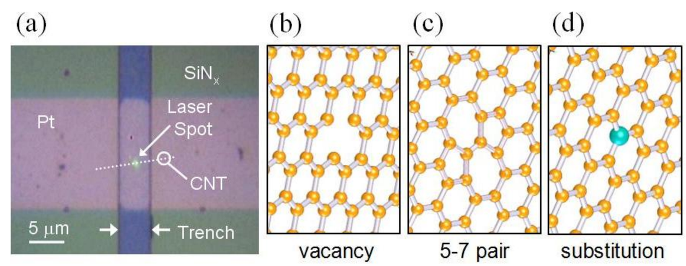

Figure 1. Device geometry and CNT defects. The microscope image of a suspended metallic single-walled CNT device used in the experiment, and possible defects in the nanotube wall: a vacancy (b), a 5-7 pair (c), and a substitutional defect (d).

II. Device Fabrication and Experimental Details

A. Chemical Vapor Deposition

Chemical vapor deposition (CVD) is used to fabricate samples with predefined catalyst sites on Pt electrodes, as reported previously [18-20]. Using this method, single-walled nanotubes were grown over trenches, thus making electrical contact with the Pt electrodes on both sides. The resulting devices were suspended with a trench depth of 300nm and a width of 5µm. The sample in this study was grown using ethanol as the carbon feedstock, and pre-selected from many potentially defected or bundled devices by careful examination of the Raman and electrical characteristics. The deviceexhibited a high bias saturation current of ~10/L (µA), where L is the length in micrometers, which indicates a single, suspended nanotube that is current-limited by optical phonon

Manuscript received November 13, 2009. This research was supported in part by DOE Award No. DE-FG02-07ER46376 and the National Science Foundation Graduate Research Fellowship Program. A portion of this work was done in the UCSB nanofabrication facility, part of the NSF funded NNIN network.

A. W. Bushmaker, C. Chang, Moh. R. Amer, and S. B. Cronin are with the University of Southern California, Los Angeles, CA 90089 USA (email: bushmake@usc.edu, chang8@usc.edu, mohammra@usc.edu, corresponding author phone: 213-740-8787; e-mail: scronin@usc.edu).

V. V. Deshpande and M. W. Bockrath were with the California Institute of Technology, Pasadena, CA 91125 USA. They are now with Columbia University, New York, NY 10027 USA and the University of California, Riverside, CA 92521 USA, respectively (email: vdesh@phys.columbia.edu, marc.bockrath@ucr.edu)

emission-induced self-heating [20]. The low temperature transport data from similar devices fabricated in this study exhibited Coulomb blockade diamonds [21]. The device showed a single, spatially isolated Raman signal, with little or no *D* band Raman intensity. These observations indicate that, initially, the nanotube in this study was a highly defect-free, individual single-walled CNT device.

B. *Laser Setup*

A 532nm laser (300µW) was focused to a diffraction-limited spot through a 100X high numerical aperture objective lens on a Leica *DM*LM microscope. This corresponds to a laser intensity of 1.5x10^5 W/cm^2. A Renishaw *InVia* spectrometer, integrated with the microscope, using 633nm excitation wavelength, collected Raman spectra. A 532nm Spectra Physics solid-state laser was used to create defects. No *D* band was observed from the nanotube throughout the course of the experiment. The focused laser-spot incident on the center of the 5µm suspended CNT can be seen in Fig. 1a.
Memristive behavior was observed in this sample, whose data are shown in Figures 2, 3, and 4. Other similar samples were exposed to the 532nm laser but were destroyed before any noticeable memristive behavior was observed. All electrical and optical measurements were performed in argon to prevent oxidation.

III. Results

A. *Defect Creation*

Fig. 2a shows the effect of laser exposure and annealing on the G-V_g profile. This nanotube initially showed a sharp dip in the conductivity near V_g = 0V, caused by the reduced carrier density in the band gap of this quasi-metallic CNT [18, 22-24]. After laser exposure, the dip in the G-V_g profile was broadened and shifted down to negative voltages, indicating a change in the local density of states. The laser spot was localized to the center of the CNT, so changes in G-V_g profile are not related to any changes in the contact resistance. When a bias voltage of V_b = 1.2V was applied to the nanotube for 15 seconds, the nanotube heated up to approximately 450^{o}C, as determined by temperature-induced downshifts in the Raman spectra [19, 25]. After this high bias annealing, we observed a partial restoring of the pristine G-V_g relationship, as shown in Fig. 2a. However, the CNT exhibited a noticeable and permanent decrease in the *p*-type conductance.

Fig. 2 also shows the change in conductivity with time during a 15-second laser exposure (Fig. 2b) and subsequent high bias annealing (Fig. 2c). A sharp drop in the conductivity was observed at the onset of laser exposure, proceeding with a time constant of approximately 10s, whereas for annealing, the change in conductivity occurred in approximately 5s following a linear time dependence. The high bias annealing of the CNT was performed in the region of negative differential conductance (NDC), as reported previously [19, 20, 26].

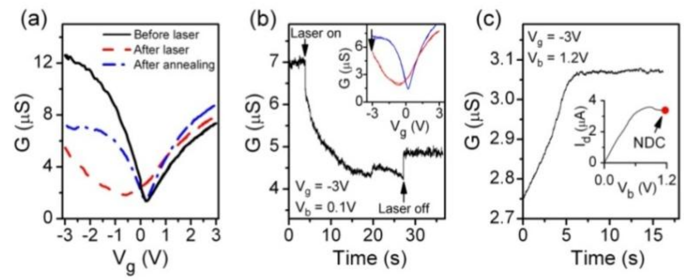

Figure 2. Conductance of a defected CNT device. (a) Low bias (V_b = 100mV) conductance versus gate voltage characteristics (G-V_g) before laser exposure, after laser exposure, and after current annealing. (b) Conductivity versus time during laser exposure and (c) subsequent high bias current annealing. Inset (b) shows the gate voltage at which the measurement was taken. Inset (c) shows the bias voltage at which the measurement was taken.

B. *Current Direction Sensitive Annealing*

Once the defect was created by laser exposure, the low bias conductivity was found to depend on the direction of the annealing current. This can be seen in Fig. 3, where the G-V_g profile is substantially different after reverse bias annealing (-V_b) as compared to that taken after forward bias annealing (+V_b). -V_b annealing of the device results in a broad G-V_g profile with a single dip centered at V_g = -0.5V. +V_b annealing, however, results in a G-V_g profile with two distinct local minima: one at V_g = -2.5V and another at V_g = 0.1V. The effects of +V_b and -V_b annealing were completely reversible, as can be seen in Fig. 3b. During annealing treatments, +V_b annealing occurred at V_g = -3V and -V_b annealing at V_g = +3V, to maintain equal carrier density. In order to rule out the gate voltage as the cause of the change, annealing was also performed with +V_b and +V_g, as well as with -V_b and -V_g. The resulting G-V_g profiles were qualitatively the same with respect to the direction of the annealing current. The power dissipation in the CNT was the same for both +V_b and -V_b annealing.

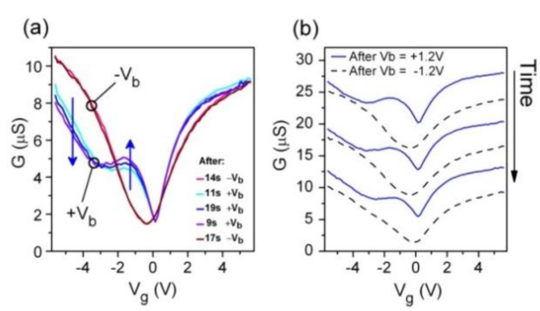

Figure 3. Repeatable switching behavior. Gate sweep conductivity profiles after successive ±1.2V bias voltage annealing show reversible switching behavior. The data in (b) are offset for clarity.

IV. Theoretical Modeling

A. Landauer Model Treatment

The data shown in Fig. 4 are fit with a Landauer transport model including the effects of a band gap, as described below. In the Landauer model [19, 20, 26-30], the nanotube resistance is expressed as

$$R = R_0^* + R_{ph} + R_d + 2R_c, \quad (1)$$

where $R_0^* = \frac{R_0}{\int_{bands} \frac{-df}{dE} dE}$, is the depleted channels' quantum resistance. Here, f is the Fermi function, $R_0 = \frac{h}{4q^2}$ is the full quantum resistance, and the integral is taken only over the electronic valence and conduction bands. R_{ph} is the resistance arising from phonon scattering in the CNT, R_d is the resistance arising from the defect, and R_c is the contact resistance. The resistance from an individual scatterer in a one-dimensional system in the Landauer model is expressed as $R = R_0^* \frac{1-T^*}{T^*}$ [31, 32], where $T^* = \frac{\int_{bands} T(E)\frac{-df}{dE} dE}{\int_{bands} \frac{-df}{dE} dE}$ is the effective transmission coefficient in the depleted quantum channels. One can see this is true by multiplying out Equation (1) for a single scatterer, as

$$R = R_0^* + R_0^* \frac{1-T^*}{T^*} = R_0^* \frac{1}{T^*}$$
$$= \frac{R_0}{\int_{bands} \frac{-df}{dE} dE} \frac{\int_{bands} \frac{-df}{dE} dE}{\int_{bands} T(E) \frac{-df}{dE} dE} = \frac{R_0}{\int_{bands} T(E) \frac{-df}{dE} dE}, \quad (2)$$

which is the result given in [32-34]. It is necessary to separate the effects of carrier depletion from those of scattering, which is done by normalizing the coefficients in the second line of Equation (2) by $\int_{bands} \frac{-df}{dE} dE$. Otherwise, the effect of carrier depletion is double-counted when considering multiple scatterers.

For phonon scattering, the transmission coefficient is $T_{ph}(E) = \frac{\lambda_{eff}(E)}{L + \lambda_{eff}(E)}$ [34]. At low bias, the electron mean free path λ_{eff} is dominated by acoustic phonon scattering mean free path. The energy dependence of the scattering rate has been examined in other studies [35]. However, here, we limit ourselves to the constant relaxation time approximation, by reducing the scattering length proportionately to the group velocity $\left(\lambda_{ac}(E) = v(E)\cdot\tau = v(E)/v_F \cdot \lambda_{ac}^{hi}\right)$, which results in short scattering lengths near the band edges [36]. λ_{ac}^{hi} was taken to be 1μm in accordance with previous work [28, 36]. The tunneling through Schottky barriers at the contacts [31, 32, 37, 38] of quasi-metallic CNTs is well approximated by a single scatterer with constant *n*-type and *p*-type transmission coefficients (T_n and T_p, respectively). These were fit separately to account for *n-p* asymmetry. Following the work by Choi et al. [7], the resonant defect state is treated as a single Lorentzian scatterer, with a transition coefficient given by

$$T_d = \frac{T_{d,0} + \left(\frac{E-E_d}{\Gamma_d}\right)^2}{1 + \left(\frac{E-E_d}{\Gamma_d}\right)^2}, \quad (3)$$

where $T_{d,0}$ is the minimum defect transmission, E_d is the energy of the defect, and Γ_d is the HWHM. We relate E_F in the nanotube to V_g by numerically solving the equation

$$E_F + \frac{Q(E_F)}{C} = eV_g, \quad (4)$$

by integrating over the density of states [22, 39]. Q is the charge induced on the nanotube, C is the geometric gate capacitance, and a hyperbolic band structure is used to model the density of states.

Using this model, the change in conductance from the forward annealed state to the reverse annealed state is interpreted as the result of a change in the atomic configuration, theoretically predicted by Choi *et al.* [7]. Mobile vacancies can reconfigure under electro-migratory pressure and, thus, change the local density of states. As seen in Fig. 4, the model qualitatively reproduces the observed change in G-V_g from that of two smaller, isolated dips in conductance (the first originating from the defect state and the second from the band gap), to one wider dip in conductance, originating from the defect with its energy shifted into the band gap. Remarkably, only small changes in fitting parameters are required other than the energy of the defect. The gate capacitance was held constant at 18 pF/m, the band gap at 110 meV, T_p = 31%, T_n = 18% for the pristine CNT and T_p = 31%, T_n = 16% for the defected CNT. For the defected CNT, the two states (forward and reverse bias annealed) have the same $T_{d,0}$ = 2.8%, with Γ_d = 400 meV for E_d = -30meV (Fig. 4b), and Γ_d = 300 meV for E_d = -180meV (Fig. 4c). The energies found here are consistent with previously reported theoretical values for vacancy type defects [7].

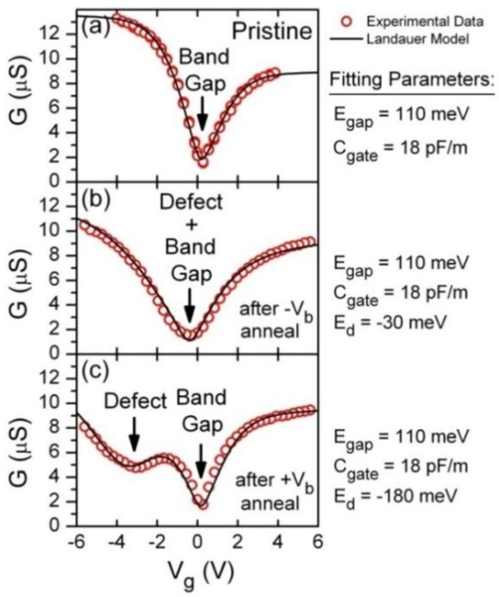

Figure 4. Landauer model fits to resonant electron scattering data. Conductance versus V_g data and Landauer model fits of a suspended nanotube device (a) before and (b,c) after laser exposure and after (b) forward and (c) reverse bias annealing. The Landauer model fitting parameters are shown on the right.

B. *Work Function*

Defects modify the local potential in CNTs [40], resulting in a non-uniform work function along the length of the nanotube. The associated inhomogeneous broadening could explain the wider G-V_g relationship observed after -V_b annealing; however, the analysis of such an effect is beyond the scope of this paper. In addition to the theory of a defect in the nanotube, non-uniform doping was also considered as the primary mechanism for this behavior, perhaps caused by local, heating-assisted desorption of surface gas molecules. This explanation relies only on thermal activation and, therefore, fails to account for the current direction-sensitive annealing behavior. Also, it is possible that the laser could be ionizing charge traps on the surface the CNT, for example, in surface-bound soot or other contaminants, which then act as local dopants and scattering sites [41]. This type of contaminant could behave like the defect discussed above, but reside on the surface of the intact CNT instead of within the wall of carbon atoms.

C. *Memristive System Equations*

Since the resistance state of the nanotube at a given V_g is dependent on the directional history of the bias current, this system falls into the general category of memristive systems [12, 13], as a time-invariant current-controlled memristive system. As such, these defected states in carbon nanotubes could potentially serve as memory elements. A general memristive system is described by the equations

$$V_b = i \cdot R(w,i) \tag{5}$$

$$dw/dt = f(w,i) \tag{6}$$

where w is the variable specifying the state of the system, $R(w,i)$ is the resistance, and $f(w,i)$ is a function describing how the state variable changes with applied current. For a true memristor, the equation is $f(w,i) = i$. In this CNT system, the energy of the defect, E_d, is the state variable, and $f(w,i)$ can be described phenomenologically with the equation

$$f(E_d,i) = dE_d/dt = \\ = \tau_0^{-1}\left\{(E_H - E_d)\exp(-i/i_{th}) + (E_L - E_d)\exp(i/i_{th})\right\}, \tag{7}$$

where E_d is the defect energy or state variable, τ_0 is the transition rate constant for crystallographic reorganization, and E_H and E_L are the high (Figure 4b) and low (Figure 4c) energy quasi-stable defect configuration states, respectively. The state variable, E_d, is then bounded by E_H and E_L. Equation (7) takes into account the self-heating temperature dependence of dE_d/dt with the exponential term and the threshold current i_{th}. The gate-tunable resistance of the system $R(i, E_d, v_g)$ is calculated using the Landauer scattering model. An interesting particularity of this memristive behavior is that, depending on the gate voltage, the resistance can be either raised or lowered (see opposing vertical arrows in Figure 3a). This third terminal control over the device polarity enables this behavior to be utilized to design devices possessing a broader range of functionalities.

V. Conclusion

In conclusion, we report current-gate voltage characteristics of a defect-induced, suspended, single-walled carbon nanotube, which displays memristive behavior. The defect is initially created by laser irradiation and is subsequently modified by annealing the nanotube with large bias currents. Forward and reverse bias current annealing results in different G-V_g characteristics, which act as a time-invariant memory element. The data is interpreted in terms of a defect state that scatters charge carriers near the defect state energy, which is sensitive to the direction of annealing currents in the nanotube. A Landauer model is used to treat the defect as an isolated scattering state in the center of the nanotube.

REFERENCES

[1] L. Chico, L. X. Benedict, S. G. Louie, and M. L. Cohen, "Quantum conductance of carbon nanotubes with defects," *Phys. Rev. B,* vol. 54, no. 4, pp. 2600-6, Jul. 1996.
[2] J. C. Charlier, T. W. Ebbesen, and P. Lambin, "Structural and electronic properties of pentagon-heptagon pair defects in carbon nanotubes," *Phys. Rev. B,* vol. 53, no. 16, pp. 11108-13, Apr. 1996.
[3] T. Kostyrko, M. Bartkowiak, and G. D. Mahan, "Reflection by defects in a tight-binding model of nanotubes," *Phys. Rev. B,* vol. 59, no. 4, pp. 3241-9, Jan. 1999.
[4] Z. Yao, H. W. C. Postma, L. Balents, and C. Dekker, "Carbon nanotube intramolecular junctions," *Nature,* vol. 402, no. 6759, pp. 273-276, Nov. 1999.
[5] L. Chico, V. H. Crespi, L. X. Benedict, S. G. Louie, and M. L. Cohen, "Pure Carbon Nanoscale Devices: Nanotube Heterojunctions," *Phys. Rev. Lett.,* vol. 76, no. 6, pp. 971-4, Feb. 1996.
[6] V. H. Crespi, M. L. Cohen, and A. Rubio, "In Situ Band Gap Engineering of Carbon Nanotubes," *Phys. Rev. Lett.,* vol. 79, no. 11, pp. 2093-6, Sep. 1997.
[7] H. J. Choi, J. Ihm, S. G. Louie, and M. L. Cohen, "Defects, Quasibound States, and Quantum Conductance in Metallic Carbon Nanotubes," *Phys. Rev. Lett.,* vol. 84, no. 13, pp. 2917-2920, Mar. 2000.
[8] J. W. Park, K. Jinhee, J. O. Lee, K. C. Kang, J. J. Kim, and K. H. Yoo, "Effects of artificial defects on the electrical transport of single-walled carbon nanotubes," *Appl. Phys. Lett.,* vol. 80, no. 1, pp. 133-135, Jan. 2002.
[9] M. Bockrath, W. Liang, D. Bozovic, J. H. Hafner, C. M. Lieber, M. Tinkham, and H. Park, "Resonant Electron Scattering by Defects in Single-Walled Carbon Nanotubes," *Science,* vol. 291, no. 5502, pp. 283-285, Jan. 2001.
[10] M. Berthe, S. Yoshida, Y. Ebine, K. Kanazawa, A. Okada, A. Taninaka, O. Takeuchi, N. Fukui, H. Shinohara, S. Suzuki, K. Sumitomo, Y. Kobayashi, B. Grandidier, D. Stievenard, and H. Shigekawa, "Reversible Defect Engineering of Single-Walled Carbon Nanotubes Using Scanning Tunneling Microscopy," *Nano Lett.,* vol. 7, no. 12, pp. 3623-3627, Nov. 2007.
[11] Z. Osvath, G. Vertesy, L. Tapaszto, F. Weber, Z. E. Horvath, J. Gyulai, and L. P. Biro, "Atomically resolved STM images of carbon nanotube defects produced by Ar[sup +] irradiation," *Phys. Rev. B,* vol. 72, no. 4, pp. 045429-34, Jul. 2005.
[12] L. O. Chua and K. Sung Mo, "Memristive devices and systems," *Proceedings of the IEEE,* vol. 64, no. 2, pp. 209-223, Feb. 1976.
[13] D. B. Strukov, G. S. Snider, D. R. Stewart, and R. S. Williams, "The missing memristor found," *Nature,* vol. 453, no. 7191, pp. 80-83, May 2008.
[14] J. J. Yang, M. D. Pickett, X. Li, A. A. OhlbergDouglas, D. R. Stewart, and R. S. Williams, "Memristive switching mechanism for metal//oxide//metal nanodevices," *Nat Nano,* vol. 3, no. 7, pp. 429-433, Jun. 2008.
[15] J. J. Yang, F. Miao, M. D. Pickett, D. A. A. Ohlberg, D. R. Stewart, C. N. Lau, and R. S. Williams, "The mechanism of electroforming of metal oxide memristive switches," *Nanotechnology,* vol. 20, pp. 215201-9, May 2009.
[16] J. Wu and R. L. McCreery, "Solid-State Electrochemistry in Molecule/TiO[sub 2] Molecular Heterojunctions as the Basis of the TiO[sub 2] ``Memristor''," *Journal of The Electrochemical Society,* vol. 156, no. 1, pp. 29-37, Nov. 2009.
[17] Y. V. Pershin and M. Di Ventra, "Spin memristive systems: Spin memory effects in semiconductor spintronics," *Phys. Rev. B,* vol. 78, no. 11, pp. 113309-4, Sep. 2008.
[18] J. Cao, Q. Wang, D. Wang, and H. Dai, "Suspended Carbon Nanotube Quantum Wires with Two Gates," *Small,* vol. 1, no. 1, pp. 138-141, Sep. 2005.
[19] A. W. Bushmaker, V. V. Deshpande, M. W. Bockrath, and S. B. Cronin, "Direct observation of mode selective electron-phonon coupling in suspended carbon nanotubes," *Nano Lett.,* vol. 7, no. 12, pp. 3618-3622, Nov. 2007.
[20] E. Pop, D. Mann, J. Cao, Q. Wang, K. Goodson, and H. Dai, "Negative Differential Conductance and Hot Phonons in Suspended Nanotube Molecular Wires," *Phys. Rev. Lett.,* vol. 95, no. 15, pp. 155505-8, Oct. 2005.
[21] V. V. Deshpande and M. Bockrath, "The one-dimensional Wigner crystal in carbon nanotubes," *Nat Phys,* vol. 4, no. 4, pp. 314-318, Mar. 2008.
[22] M. J. Biercuk, S. Ilani, C. M. Marcus, and P. L. McEuen, "Electrical Transport in Single-Wall Carbon Nanotubes," *Topics in Applied Physics,* vol. 111, pp. 455-93, 2008.
[23] M. Ouyang, J.-L. Huang, C. L. Cheung, and C. M. Lieber, "Energy Gaps in "Metallic" Single-Walled Carbon Nanotubes," *Science,* vol. 292, no. 5517, pp. 702-705, Apr. 2001.
[24] V. V. Deshpande, B. Chandra, R. Caldwell, D. S. Novikov, J. Hone, and M. Bockrath, "Mott Insulating State in Ultraclean Carbon Nanotubes," *Science,* vol. 323, no. 5910, pp. 106-110, Jan. 2009.
[25] H. D. Li, K. T. Yue, Z. L. Lian, Y. Zhan, L. X. Zhou, S. L. Zhang, Z. J. Shi, Z. N. Gu, B. B. Liu, R. S. Yang, H. B. Yang, G. T. Zou, Y. Zhang, and S. Iijima, "Temperature dependence of the Raman spectra of single-wall carbon nanotubes," *Appl. Phys. Lett.,* vol. 76, no. 15, pp. 2053-2055, Apr. 2000.
[26] M. Lazzeri, S. Piscanec, F. Mauri, A. C. Ferrari, and J. Robertson, "Electron Transport and Hot Phonons in Carbon Nanotubes," *Phys. Rev. Lett.,* vol. 95, pp. 236802-5, Nov. 2005.
[27] D. Mann, E. Pop, J. Cao, Q. Wang, K. Goodson, and H. Dai, "Thermally and Molecularly Stimulated Relaxation of Hot Phonons in Suspended Carbon Nanotubes," *J. Phys. Chem. B Lett.,* vol. 110, no. 4, pp. 1502-1505, Jan. 2006.
[28] J. Y. Park, S. Rosenblatt, Y. Yaish, V. Sazonova, H. Ustunel, S. Braig, T. A. Arias, P. W. Brouwer, and P. L. McEuen, "Electron-Phonon Scattering in Metallic Single-Walled Carbon Nanotubes," *Nano Lett.,* vol. 4, no. 3, p. 517, 2003.
[29] Z. Yao, C. L. Kane, and C. Dekker, "High-Field Electrical Transport in Single-Wall Carbon Nanotubes," *Phys. Rev. Lett.,* vol. 84, no. 13, p. 2941, Mar. 2000.
[30] A. W. Bushmaker, V. V. Deshpande, S. Hsieh, M. W. Bockrath, and S. B. Cronin, "Gate Voltage Controllable Non-Equilibrium and Non-Ohmic Behavior in Suspended Carbon Nanotubes," *Nano Lett.,* vol. 9, no. 8, pp. 2862-2866, Jul. 2009.
[31] A. Bachtold, M. S. Fuhrer, S. Plyasunov, M. Forero, E. H. Anderson, A. Zettl, and P. L. McEuen, "Scanned Probe Microscopy of Electronic Transport in Carbon Nanotubes," *Phys. Rev. Lett.,* vol. 84, no. 26, p. 6082, Jun. 2000.
[32] A. Buldum and J. P. Lu, "Contact resistance between carbon nanotubes," *Phys. Rev. B,* vol. 63, no. 16, pp. 161403-6, Apr. 2001.
[33] Y. Zhao, A. Liao, and E. Pop, "Multiband Mobility in Semiconducting Carbon Nanotubes," *IEEE electron device letters,* vol. 30, no. 10, pp. 1078-1080, 2009.
[34] T. Seri and T. Ando, "Boltzmann Conductivity of a Carbon Nanotube in Magnetic Fields," *Journal of the Physical Society of Japan,* vol. 66, no. 1, pp. 169-173, Jan. 1997.
[35] V. Perebeinos, J. Tersoff, and P. Avouris, "Electron-Phonon Interaction and Transport in Semiconducting Carbon Nanotubes," *Phys. Rev. Lett.,* vol. 94, no. 8, p. 086802, Mar. 2005.
[36] S. O. Koswatta, S. Hasan, M. S. Lundstrom, M. P. Anantram, and D. E. Nikonov, "Ballisticity of nanotube field-effect transistors: Role of phonon energy and gate bias," *Appl. Phys. Lett.,* vol. 89, no. 2, pp. 023125-3, Jul. 2006.
[37] R. Martel, V. Derycke, C. Lavoie, J. Appenzeller, K. K. Chan, J. Tersoff, and P. Avouris, "Ambipolar Electrical Transport in Semiconducting Single-Wall Carbon Nanotubes," *Phys. Rev. Lett.,* vol. 87, no. 25, p. 256805, Dec. 2001.
[38] V. Derycke, R. Martel, J. Appenzeller, and P. Avouris, "Controlling doping and carrier injection in carbon nanotube transistors," *Appl. Phys. Lett.,* vol. 80, no. 15, pp. 2773-2775, Apr. 2002.
[39] A. Das, S. Pisana, B. Chakraborty, S. Piscanec, S. K. Saha, U. V. Waghmare, K. S. Novoselov, H. R. Krishnamurthy, A. K. Geim, A. C. Ferrari, and A. K. Sood, "Monitoring dopants by Raman scattering in an electrochemically top-gated graphene transistor," *Nat. Nano.,* vol. 3, no. 4, pp. 210-215, Mar. 2008.
[40] K. Balasubramanian, M. Burghard, K. Kern, M. Scolari, and A. Mews, "Photocurrent Imaging of Charge Transport Barriers in Carbon Nanotube Devices," *Nano Lett,* vol. 5, no. 3, pp. 507-510, Feb. 2005.
[41] J. M. Simmons, I. In, V. E. Campbell, T. J. Mark, F. Leonard, P. Gopalan, and M. A. Eriksson, "Optically modulated conduction in chromophore-functionalized single-wall carbon nanotubes," *Phys. Rev. Lett.,* vol. 98, no. 8, pp. 86802-5, Feb. 2007.